

Article

Isolation and Characterization of Two Novel Lytic Bacteriophages against *Salmonella typhimurium* and Their Biocontrol Potential in Food Products

Yaxiong Song , Wentao Gu, Yaozhong Hu , Bowei Zhang, Jin Wang, Yi Sun, Wenhui Fu, Xinyang Li , Xiaolong Xing and Shuo Wang *

Tianjin Key Laboratory of Food Science and Health, School of Medicine, Nankai University, Tianjin 300071, China; ysong90@nankai.edu.cn (Y.S.); kt1667mail@163.com (W.G.); yzhu@nankai.edu.cn (Y.H.); bwzhang@nankai.edu.cn (B.Z.); wangjin@nankai.edu.cn (J.W.); 9920220161@nankai.edu.cn (Y.S.); ahfyfwh@163.com (W.F.); lixinyang@nankai.edu.cn (X.L.); xingxl@nankai.edu.cn (X.X.)

* Correspondence: wangshuo@nankai.edu.cn

Abstract: Foodborne pathogens, such as *Salmonella*, are major factors that pose significant threats to global food safety and public health. *Salmonella typhimurium* is a prominent serotype contributing to non-typhoidal salmonellosis, which is a prevalent foodborne illness affecting humans and animals. Bacteriophages are considered one of the most environmentally friendly biocontrol agents, particularly in the food industry, owing to their high specificity and high safety. However, the emergency of phage-resistant mutants limits the biocontrol effect of phage treatment, leading to the requirement for a high diversity of lytic phages. Therefore, the study isolated and characterized two novel lytic *Salmonella* bacteriophages (SPYS_1 and SPYS_2) targeting *S. typhimurium* ATCC14028 and evaluated their effectiveness in reducing the contamination rates for milk and chicken tenders. Morphological and genomic analyses indicated that *Salmonella* phages SPYS_1 and SPYS_2 are novel species classified under the genus *Skatevirus* and the genus *Berlinvirus*, respectively. Both phages exhibited high stability across a broad range of thermal and pH conditions. The one-step growth curve result suggested that both phages had a short adsorption time and a large burst size in a single lytic cycle. The phage SPYS_1 demonstrated a noteworthy inhibition effect on the growth of *S. typhimurium* ATCC14028 in milk, resulting in a ~2-log reduction within the 2 to 4 h range. Overall, both phages have shown significant potential for application in food safety in the future.

Keywords: *Salmonella typhimurium*; bacteriophages; food application; food safety; biocontrol



Citation: Song, Y.; Gu, W.; Hu, Y.; Zhang, B.; Wang, J.; Sun, Y.; Fu, W.; Li, X.; Xing, X.; Wang, S. Isolation and Characterization of Two Novel Lytic Bacteriophages against *Salmonella typhimurium* and Their Biocontrol Potential in Food Products. *Foods* **2024**, *13*, 3103. <https://doi.org/10.3390/foods13193103>

Academic Editor: Baotao Liu

Received: 29 August 2024

Revised: 23 September 2024

Accepted: 25 September 2024

Published: 28 September 2024



Copyright: © 2024 by the authors. Licensee MDPI, Basel, Switzerland. This article is an open access article distributed under the terms and conditions of the Creative Commons Attribution (CC BY) license (<https://creativecommons.org/licenses/by/4.0/>).

1. Introduction

Salmonella is one of the major foodborne pathogens that threaten public health in the world [1–3]. After the ingestion of contaminated food or water, *Salmonella* colonizes the gastrointestinal tract and causes salmonellosis, which is characterized by symptoms such as diarrhea, fever, and abdominal cramps [2,4,5]. *Salmonella* can be grouped into over 2600 serotypes regarding the surface antigenic determinants with certain serotypes acting as zoonotic pathogens that can infect both humans and animals [3,6,7]. *S. typhimurium* is one of the most isolated serotypes responsible for self-limiting gastroenteritis, which is identified as one of the non-typhoidal *salmonellae* [8–10]. It is estimated that 93.8 million non-typhoidal *Salmonella* gastroenteritis cases occur every year globally with ~155,000 deaths [11,12]. In the United States, the economic losses associated with non-typhoidal *salmonellae* infection exceeded USD 4.14 billion with 1,027,561 infection cases in 2018 [13,14].

In the food industry, various disinfection technologies are employed in food processing and preservation, including chemical agents, thermal treatment, irradiation treatment, etc. [15–18]. However, the flavor, color, and nutritional quality of food are easily negatively

affected by the current decontamination method [15]. To ensure food quality and safety, an effective technology without adverse impact is urgently needed [19].

Bacteriophages (phages) are natural antibacterial viruses that are considered as promising alternatives to antibiotics for biocontrolling pathogens in the food industry [15,17,20]. Due to their high specificity, phages exert no influence on food quality and safety, as they only infect and lyse their host strains [15,21]. Consequently, phages are increasingly accepted by the public as environment-friendly antimicrobial agents, and several commercial phage products have been utilized for decades to biocontrol *Salmonella* contamination [22]. Nevertheless, a primary challenge in phage-based biocontrol is the emergence of phage-resistant mutants [23]. To address this issue, employing a diverse of phages to broaden the host range could be an effective solution [24,25]. Therefore, it is crucial to isolate more *Salmonella* phages to establish a robust foundation for the application in the future.

This study aims to isolate and characterize novel lytic bacteriophages targeting *S. typhimurium*. Consequently, *Salmonella* phages SPYS_1 and SPYS_2 were isolated from local market sewage and identified as novel species through morphological and genomic analyses, demonstrating a high tolerance to environmental stress. We further assessed the biocontrol effect of the isolated phages on milk and chicken tenders, indicating significant potential for food safety applications.

2. Materials and Methods

2.1. Bacterial Strains and Growth Conditions

S. typhimurium ATCC 14028 was used as the host strain throughout the processes of phage isolation, purification, and propagation. A total of 12 standard *Salmonella* strains were used for the Efficient of Plaques experiment (EOP), which was generously provided by Professor Yongping Xu in Dalian University of Technology (Table 1). All *Salmonella* strains were stored at $-80\text{ }^{\circ}\text{C}$ in Luria–Bertani (LB) broth supplemented with 15% (*v/v*) glycerol.

Table 1. *Salmonella* strains.

Strain ID Number	Species	Serovar
ATCC14028 ^a	<i>Salmonella enterica</i>	Typhimurium
CMCC50115 ^b	<i>Salmonella enterica</i>	Typhimurium
CMCC50220	<i>Salmonella enterica</i>	Typhimurium
CICC21484 ^c	<i>Salmonella enterica</i>	Typhimurium
ATCC25241	<i>Salmonella enterica</i>	Typhimurium
CICC10437	<i>Salmonella enterica</i>	Paratyphi B
CICC21501	<i>Salmonella enterica</i>	Paratyphi A
CICC10871	<i>Salmonella enterica</i>	Typhi
CVCC3378 ^d	<i>Salmonella enterica</i>	Typhi
CICC21510	<i>Salmonella enterica</i>	Gallinarum
CVCC3383	<i>Salmonella enterica</i>	choleraesuis
CVCC503	<i>Salmonella enterica</i>	choleraesuis
CVCC79102	<i>Salmonella enterica</i>	choleraesuis

^a ATCC stands for The American Type Culture Collection (<https://www.atcc.org/>, accessed date 5 August 2024);

^b CMCC stands for National Center for Medical Culture Collections (<https://www.cmccb.org.cn>, accessed date 5 August 2024); ^c CICC stands for China Center of Industrial Culture Collection (<http://english.china-cicc.org>,

accessed date 5 August 2024); ^d CVCC stands for National Center for Veterinary Culture Collections (<http://cvcc.ivdc.org.cn>, accessed date 5 August 2024).

All *Salmonella* strains were streaked onto 1.5% (*w/v*) LB agar plates and cultured at $37\text{ }^{\circ}\text{C}$. *Salmonella* strains were activated by taking a single colony from the streak plate into LB broth and incubating it at $37\text{ }^{\circ}\text{C}$, shaking at 160 RPM for 16–20 h.

2.2. Phage Isolation, Purification, and Propagation

Sewage samples were obtained from a wet market in Tianjin, China. Samples were placed in 50 mL sterile centrifuge tubes and kept in ice boxes at $4\text{ }^{\circ}\text{C}$ during transport.

They were subsequently centrifuged at $5000\times g$ and $4\text{ }^{\circ}\text{C}$ for 20 min to remove solid debris. After centrifugation, the supernatants were filtered through $0.20\text{ }\mu\text{m}$ syringe filters. To enrich potential phages in the samples, a mixture of 10 mL of each treated sample, 10 mL of $2\times$ LB broth, and 1 mL of an overnight culture of *S. typhimurium* ATCC 14028 was incubated at $37\text{ }^{\circ}\text{C}$ with shaking at 160 RPM for 16–20 h. After the incubation, the medium was re-treated through centrifugation and filtration using the same process as employed for the sewage samples. The presence of phages in samples was verified by the double-layer method, showing clear plaques on the host strain. For this method, a $100\text{ }\mu\text{L}$ enriched sample and $100\text{ }\mu\text{L}$ overnight culture of host strain were mixed in 3 mL 0.7% (w/v) top LB agar (supplemented with 1 mM CaCl_2 and 1 mM MgCl_2) at $55\text{ }^{\circ}\text{C}$ and poured onto the 1.5% (w/v) LB agar plates, which was followed by incubation at $37\text{ }^{\circ}\text{C}$ for 16–20 h.

After phage isolation, a distinct plaque was transferred and resuspended into 1 mL Salt Magnesium (SM) buffer for 24 h. The morphology of the purified phages was then observed using the double-layer method. The purification of phages was subjected to at least three passages until plaques on the plate exhibited a consistent size and shape.

Following phage purification, the phages were prepared for propagation using the plate lysate method for initial enrichment. In this method, purified phages ($\sim 10^4$ PFU) and a $100\text{ }\mu\text{L}$ overnight culture of host strain were mixed in 3 mL 0.7% (w/v) top LB agar (supplemented with 1 mM CaCl_2 and 1 mM MgCl_2) at $55\text{ }^{\circ}\text{C}$ and poured onto the 1.5% (w/v) LB agar plates, incubating at $37\text{ }^{\circ}\text{C}$ for 16–20 h. Then, we added 5 mL SM buffer onto each plate with confluent lysis and let the plates stand at room temperature for 1–2 h. Using cell scrapers to chop up the top agar layer and collect as much liquid as possible, we then centrifuged at $1000\times g$, $4\text{ }^{\circ}\text{C}$, for 15 min. The supernatant was filtered through $0.20\text{ }\mu\text{m}$ filters and titered by the spot assay method.

A high titer ($\sim 10^9$ PFU/mL) of phage stocks was attained through the plate lysed method, which was followed by the liquid amplification method for a higher titer. For liquid amplification, 1 mL of overnight culture of *S. typhimurium* ATCC 14028 was added into 50 mL LB liquid broth (supplemented with 1 mM CaCl_2 and 1 mM MgCl_2), incubating at $37\text{ }^{\circ}\text{C}$, shaking at 160 RPM. When the optical density at 600 nm ($\text{OD}_{600\text{nm}}$) grew to approximately 0.3, purified phages were added with a multiplicity of infection (MOI) of ~ 0.1 and incubated at $37\text{ }^{\circ}\text{C}$, shaking at 160 RPM for 3 h. After incubation, the culture was treated by 5% (v/v) chloroform at room temperature for at least 15 min, and the aqueous phase was then centrifuged at $5000\times g$, $4\text{ }^{\circ}\text{C}$, for 20 min. Following centrifugation, supernatants were centrifuged at $12,000\times g$, $4\text{ }^{\circ}\text{C}$, for 2 h, and then the precipitation was covered by 5 mL SM buffer for 24 h. Finally, the precipitation was resuspended in SM buffer and filtered with $0.20\text{ }\mu\text{m}$ syringe filters. The titer of the phage lysate was measured by the double-layer method.

2.3. Morphological Observation of Phage by Transmission Electron Microscopy (TEM)

A volume of $20\text{ }\mu\text{L}$ high-titer ($\sim 10^{10}$ PFU/mL) phage samples was deposited onto 200-mesh grids and allowed to incubate at room temperature for 10 min; then, the grids were negative stained for 3 min using 2% phosphotungstic acid, and the remaining liquid was removed with filter paper. After staining, the phage samples were imaged on a JEOL JEM1400 transmission electron microscopy (JEOL LTD, Tokyo, Japan). The images were processed with Adobe Illustrator CC 2018. Ten representative samples of each phage were selected to measure the size through ImageJ (version 1.54g).

2.4. DNA Extraction and Genome Analysis

The genomic DNA of the isolated phages was extracted with a Lambda phage Genomic DNA Kit (Zoman Biotechnology, Beijing, China), following the manufacturer's guidelines. The concentration and quality of DNA samples were measured by a Nanodrop spectrophotometer (ThermoFisher Scientific, Waltham, MA, USA) before sequencing.

Phage DNA raw reads were obtained by Illumina sequencing. For a high-quality clean read, raw reads were filtered through by Soapnuke (v2.0.5) [26]. Then, BWA (v0.7.17) [27]

was employed to remove host contamination. Phage genome assemblies were conducted through de novo assembly using Megahit (v1.1.2) [28], and the utilization rate of reads was calculated by BWA (v0.7.17). Taxonomic predictions for the isolated phages were made by comparing the virus library with checkv (v1.0) [29]. Whether the structure of the phage genome is circular was determined by using ccfind (v1.4.5) [30]. The lifestyle was predicted by PhaTYP (<https://phage.ee.cityu.edu.hk/phabox>, accessed on 30 August 2023) [31]. JspeciesWS [32] was adopted to analyze the similarity of isolated phages with other *Skatevirus* or *Berlinvirus* by the average nucleotide identity MUMer (ANIm) method [33,34]. The phage genome was annotated using RASTtk (v1.3.0) [35], and annotations were subsequently manually modified and supplemented through Uniprot (<https://www.uniprot.org/>, accessed on 4 September 2023). The genome maps of the isolated phage were generated with updated annotations using Proksee (<https://proksee.ca/>, accessed on 4 September 2023) [36].

2.5. Efficiencies of Plaquing

S. typhimurium ATCC 14028 and 12 other standard *Salmonella* strains were used to conduct efficiency of plaquing (EOP) as previously described (Table 1) [24,37]. Briefly, all phages were diluted to $\sim 10^8$ PFU/mL as working stocks, and the titers of working stocks on each *Salmonella* strain were measured by the spot assay method. The EOP for each phage on each strain represented the relative value of the titer compared to the highest titer of that specific phage across all strains. The EOP heatmap was generated using *heatmap* package in R (v4.3.3) [38].

2.6. Phage Stability Test

The stability of the isolated phages was assessed by monitoring changes in titers under various culture conditions, including chloroform treatment, different temperatures and different pH.

The phage stocks that were achieved from the plate lysate method were adopted for the chloroform stability test, as these phages were not subjected to chloroform treatment during propagation. Five microliters of chloroform were added into 1 mL phage stock and allowed to stand for 1 h at room temperature. The titers of both untreated phages and phages treated with chloroform were measured by the spot assay method.

The thermal stress stability of the phage was evaluated by incubating phages under different temperatures (4 °C, 37 °C, 50 °C, 60 °C, 70 °C, 80 °C) for 1 h. After incubation, the titers of the phages at different temperatures were measured using the spot assay method.

The pH stress stability of the phages was assessed by inoculating the phage stocks into 1 mL SM buffer adjusted to different pH levels (ranging from pH 2.0 to 13.0) and incubating them at 4 °C for 24 h. After incubation, the titers of phage in different pH levels were measured using the spot assay method.

2.7. One-Step Growth Experiment

One-step growth curve experiments were performed as previously described with modifications [24]. One milliliter of overnight culture of the host strain was added into 50 mL LB broth (supplemented with 1 mM CaCl₂ and 1 mM MgCl₂). The culture was incubated at 37 °C, shaking at 160 RPM until the concentration of the host strain reached $\sim 10^8$ CFU/mL (OD_{600nm} ~ 0.3). Then, the culture was infected with the isolated phage at a multiplicity of infection (MOI) of 0.1. The infected culture was incubated at 37 °C, shaking at 160 RPM for 3 h, and we collected two samples at each time point. One sample was immediately enumerated using the spot assay method, while the other sample was treated with 5% (v/v) chloroform for at least 15 min before enumeration by the spot assay method, allowing to measure infected host cells and unabsorbed viable phages.

2.8. Growth Inhibition Experiment

The exponential-phase culture of the *S. typhimurium* ATCC 14028 was infected with either a single isolated phage or a mixture of phages at an MOI of 0.1, 1, and 10, evaluating the inhibition effort of the phages in vitro. SM buffer was added as the negative control. The OD_{600nm} of each culture was measured at each point in time.

2.9. Biocontrol Effect of the Isolated Phages against *Salmonella* in Food

Pasteurized milk and chicken tenders were purchased from a local supermarket for the purpose of assessing the biocontrol effect against *Salmonella* in food. Before the experiment, the pasteurized milk was stored at 4 °C, and the chicken tenders were stored at −20 °C. An exponential-phase culture of *S. typhimurium* ATCC 14028 (~10⁸ CFU/mL) was prepared for the experiment, and the phage stocks were diluted into ~10⁷ PFU/mL as working stock; SM buffer was used as the negative control. Since the optimum MOI determined in the broth test was 0.1, this dosage was also applied in the food application experiment to maintain consistency and effectiveness.

The inhibition effect of phage against *Salmonella* in milk was evaluated by mixing 20 µL phage working stock and 20 µL *S. typhimurium* ATCC 14028 in 19.96 mL pasteurized milk. The mixture was then incubated at 37 °C with shaking at 160 RPM for 48 h. At each time point, 500 µL samples were taken and centrifuged at 5000 × g for 5 min. The concentration of the host strain was enumerated after the precipitate was resuspended by 500 µL phosphate-buffered saline (PBS).

The inhibitory effect of the phage against *Salmonella* in chicken tenders was assessed by applying 100 µL of the phage working stock to the surface of the sample contaminated with *S. typhimurium* ATCC 14028 and incubating at 37 °C for 48 h. Before the experiment, the chicken tenders were cut into 1 cm³ cubes, and the surfaces of each cube were washed with 75% ethanol, which was followed by air drying. Then, the chicken samples were sterilized using UV light for one hour with a midway rotation. Following the disinfection process, the host strain and phage working stock were sequentially deposited at 15-min intervals, allowing for the air drying of the *Salmonella* strain. At each time point, a chicken cube in each treatment group was fully immersed in PBS, followed by a one-minute high-speed vortex treatment, and the concentration of the host strain in the supernatant was enumerated.

2.10. Statistical Analysis

All experiments were performed with three biological replicates unless specifically stated, and the data are shown as means ± standard deviation (SD). Significance differences among groups were assessed in the phage stability test and food application experiment using the Student–Newman–Keuls test. A *p*-value < 0.05 was considered statistically significant.

3. Results

3.1. Isolation and Characterization of Phage SPYS_1 and SPYS_2

3.1.1. Isolation of *Salmonella* Phages

In this study, a total of 10 sewage samples were collected from a wet market in Tianjin. After isolation and purification, two *Salmonella* phages (SPYS_1 and SPYS_2) showed consistent ability to form plaques on *S. typhimurium* ATCC 14028 and were thus identified as potential agents to biocontrol *Salmonella* contamination in food for further research.

3.1.2. Morphology Analysis by TEM Imaging

The TEM images of SPYS_1 and SPYS_2 revealed two distinct morphologies. *Salmonella* phage SPYS_1 has an icosahedron head with a long, rigid tail, belonging to the family *Siphoviridae* in the order of *Caudovirales* (Figure 1A). The capsid of *Salmonella* phage SPYS_1 is 58.30 ± 5.04 nm in diameter, while the tail is 133.15 ± 8.65 nm in length and 11.37 ± 2.63 nm in width (Figure 1A). *Salmonella* phage SPYS_2 has an icosahedron head

with a short tail, belonging to the family *Autographiviridae* in the order of *Caudovirales* (Figure 1B). The capsid of *Salmonella* phage SPYS_2 is 54.32 ± 5.37 nm in diameter, while the tail is 11.67 ± 3.46 nm in length and 10.07 ± 3.99 nm in width (Figure 1B).

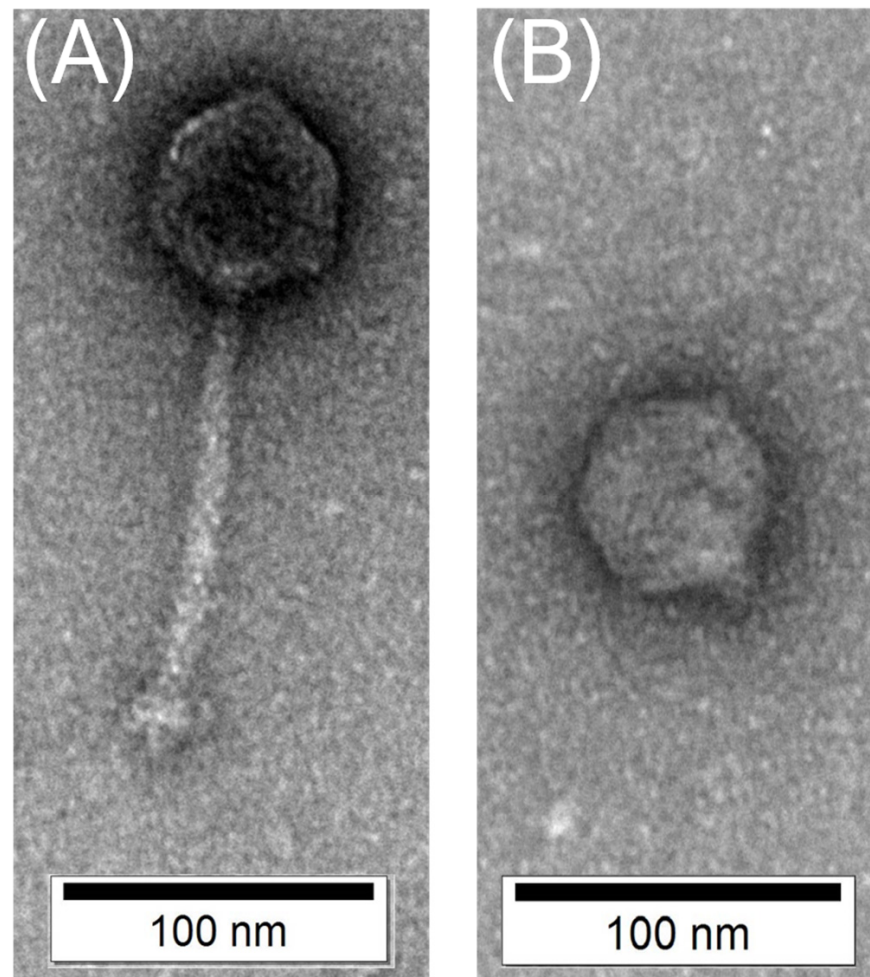


Figure 1. Transmission electron microscopy images of two *Salmonella* phages targeting *S. typhimurium* ATCC 14028. (A) *Salmonella* phage SPYS_1 has an icosahedron head with a long, rigid tail; (B) *Salmonella* phage SPYS_2 has an icosahedron head with a short tail. Phages were stained with 2% phosphotungstic acid and imaged on a JEOL JEM1400 transmission electron microscopy.

3.1.3. Genome Analysis of *Salmonella* Phage SPYS_1 and SPYS_2

The complete genomes of *Salmonella* phages SPYS_1 and SPYS_2 have been sequenced and submitted to NCBI with the accession number PRJNA1051981.

The raw reads of *Salmonella* phages SPYS_1 and SPYS_2 were assembled into single contigs, respectively. Assembly results revealed that the genome of *Salmonella* phage SPYS_1 has a circular dsDNA genome composed of 45,220 bp with a GC content of 45.98% (Figure 2A), and the genome of *Salmonella* phage SPYS_2 has a circular dsDNA genome composed of 40,079 bp with a GC content of 48.45% (Figure 2B). The genome of *Salmonella* phage SPYS_1 contains 82 coding sequences (CDS) with 39 annotated as hypothetical proteins (Figure 2A). The genome of *Salmonella* phage SPYS_2 contains 49 coding sequences (CDS) with 14 annotated as hypothetical proteins (Figure 2B). *Salmonella* phage SPYS_1 and SPYS_2 were both predicted to have a virulent lifestyle by PhaTYP analysis.

Table 2. Jspecies results for *Salmonella* phage SPYS_1 with other *Skatevirus* phages.

Phage	Average Nucleotide Identity (ANI; %) [Aligned Nucleotides (%)]													
	Salmonella Phage SPYS_1	Salmonella Phage D10	Salmonella Phage INT55	Salmonella Phage INT59	Salmonella Phage LPST10	Salmonella Phage Pu29	Salmonella Phage SeSz-2	Salmonella Phage Sesz_1	Salmonella Phage Sezh_1	Salmonella Phage Skate	Salmonella Phage VB_StyS_BS5	Salmonella Virus KFS-SE2	Salmonella Virus SeLz-2	Salmonella Virus VSt472
Salmonella phage SPYS_1	-	90.92 [62.28]	86.55 [61.69]	86.54 [61.69]	90.79 [62.22]	90.92 [61.95]	90.16 [64.57]	89.97 [66.89]	86.68 [60.14]	91.73 [70.66]	90.44 [57.74]	85.61 [63.45]	92.40 [62.44]	89.25 [62.16]
Salmonella phage D10	88.24 [64.04]	-	86.85 [56.20]	86.79 [56.29]	92.06 [65.88]	100.00 [96.61]	95.89 [79.98]	86.50 [57.25]	87.62 [60.69]	87.71 [64.18]	90.68 [67.81]	87.13 [64.56]	87.41 [54.14]	90.69 [61.76]
Salmonella phage INT55	86.47 [65.56]	87.57 [62.10]	-	99.99 [99.61]	88.82 [68.45]	87.61 [61.23]	87.89 [67.42]	88.14 [67.21]	86.13 [61.98]	87.08 [67.95]	89.52 [65.07]	87.18 [68.99]	87.45 [57.17]	88.45 [60.53]
Salmonella phage INT59	86.46 [66.92]	87.34 [62.62]	99.99 [99.51]	-	88.81 [68.49]	87.37 [61.77]	87.62 [67.92]	87.49 [70.03]	86.15 [62.15]	86.93 [68.22]	89.55 [65.19]	86.99 [69.41]	87.30 [57.52]	88.39 [60.68]
Salmonella phage LPST10	89.81 [61.02]	92.23 [67.97]	88.81 [65.11]	88.76 [65.21]	-	92.09 [65.83]	88.94 [60.96]	88.67 [59.67]	88.99 [76.03]	88.43 [61.55]	96.15 [76.45]	88.67 [62.56]	87.77 [55.11]	93.14 [71.09]
Salmonella phage Pu29	88.90 [63.67]	100.00 [95.49]	86.95 [60.78]	86.91 [60.86]	92.47 [71.73]	-	96.09 [78.63]	87.82 [59.46]	87.85 [67.82]	87.45 [69.63]	91.41 [67.23]	87.34 [69.24]	86.52 [62.33]	91.11 [67.31]
Salmonella phage SeSz-2	89.16 [64.47]	96.21 [78.67]	87.27 [66.00]	87.27 [66.00]	89.41 [60.00]	96.65 [78.81]	-	88.42 [55.32]	89.12 [64.18]	88.19 [65.47]	88.84 [61.54]	85.98 [67.25]	89.52 [58.40]	89.81 [64.11]
Salmonella phage Sesz_1	90.01 [64.77]	86.87 [61.59]	88.71 [64.64]	88.71 [64.64]	88.25 [63.39]	86.81 [61.66]	88.62 [60.34]	-	85.58 [60.95]	92.64 [63.00]	89.80 [66.80]	87.78 [57.04]	91.54 [59.30]	89.39 [61.75]
Salmonella phage Sezh_1	87.71 [50.51]	88.30 [60.43]	86.48 [55.42]	86.47 [55.42]	89.60 [70.04]	88.30 [60.43]	89.11 [57.38]	86.42 [51.38]	-	86.02 [51.05]	88.15 [60.33]	85.16 [56.80]	86.27 [48.01]	88.61 [54.67]
Salmonella phage Skate	92.20 [60.35]	88.22 [60.64]	87.03 [64.68]	87.02 [64.68]	88.95 [63.53]	88.22 [60.64]	88.64 [62.56]	92.13 [64.21]	87.18 [59.28]	-	89.18 [64.69]	88.63 [67.24]	94.04 [68.61]	88.13 [63.38]
Salmonella phage VB_StyS_BS5	88.19 [58.04]	90.38 [64.26]	87.70 [63.60]	87.70 [63.60]	96.13 [71.57]	90.38 [64.26]	88.26 [60.02]	90.78 [59.74]	88.99 [61.59]	88.19 [62.60]	-	88.23 [59.28]	87.03 [55.37]	93.19 [68.73]
Salmonella virus KFS-SE2	86.12 [62.27]	86.91 [64.62]	87.89 [61.05]	87.89 [61.05]	88.13 [61.15]	86.89 [64.40]	86.78 [58.75]	88.79 [57.26]	85.89 [59.72]	88.01 [63.17]	87.77 [61.69]	-	86.28 [60.54]	87.99 [70.52]
Salmonella virus SeLz-2	92.35 [72.76]	86.69 [65.50]	87.10 [62.86]	87.09 [62.88]	87.80 [63.43]	86.83 [65.32]	88.25 [68.80]	90.81 [69.33]	85.42 [63.24]	97.03 [69.27]	87.55 [62.56]	84.51 [68.18]	-	87.52 [65.90]
Salmonella virus VSt472	87.44 [64.95]	90.62 [62.27]	87.69 [59.84]	87.68 [59.86]	93.20 [67.32]	90.62 [62.27]	89.14 [64.05]	88.95 [62.93]	90.33 [58.56]	87.66 [59.73]	93.31 [68.72]	87.57 [67.33]	88.29 [55.12]	-

Table 3. Jspecies results for *Salmonella* phage SPYS_2 with other *Berlinovirus* phages.

Phage	Average Nucleotide Identity (ANI; %) [Aligned Nucleotides (%)]										
	Salmonella Phage SPYS_2	Salmonella Phage BP12A	Salmonella Phage BSP161	Salmonella Phage JSS1	Salmonella Phage JSS2	Salmonella Phage LPST144	Salmonella Phage SWJM-03	Salmonella Phage vB_SalM_PC127	Salmonella Phage vB_SalM- LPST153	Salmonella Phage vB_SalS_PC192	Salmonella Phage vB_STy-RN5i1
Salmonella phage SPYS_2	-	86.74 [84.07]	91.05 [75.45]	88.03 [77.62]	86.76 [80.64]	85.75 [84.83]	86.03 [84.34]	92.26 [85.41]	85.80 [84.22]	92.44 [84.09]	92.66 [80.65]
Salmonella phage BP12A	87.28 [79.49]	-	87.56 [76.22]	87.97 [85.26]	88.16 [81.13]	92.91 [86.28]	93.31 [88.56]	86.80 [78.24]	92.90 [85.68]	86.79 [79.29]	87.11 [81.96]
Salmonella phage BSP161	91.36 [74.39]	89.11 [77.05]	-	89.72 [77.03]	88.09 [80.16]	87.42 [80.73]	88.06 [79.44]	90.50 [72.16]	87.38 [79.90]	90.74 [74.27]	92.15 [73.23]
Salmonella phage JSS1	88.94 [74.91]	88.23 [81.27]	89.55 [77.63]	-	89.81 [79.11]	87.16 [75.00]	87.16 [80.56]	89.09 [66.30]	87.19 [74.42]	89.17 [67.05]	88.73 [72.27]
Salmonella phage JSS2	87.46 [80.40]	88.41 [87.44]	87.10 [85.71]	89.01 [88.48]	-	91.37 [92.20]	89.79 [87.07]	87.66 [77.04]	91.41 [91.95]	87.68 [77.64]	87.56 [76.49]
Salmonella phage LPST144	86.56 [84.96]	93.48 [88.06]	86.04 [83.84]	86.90 [80.17]	90.85 [92.70]	-	96.17 [89.41]	86.15 [77.64]	99.98 [98.80]	86.50 [79.26]	87.11 [77.63]
Salmonella phage SWJM-03	86.30 [82.15]	93.34 [88.32]	86.59 [82.79]	87.22 [87.15]	89.19 [85.24]	95.88 [89.61]	-	86.17 [80.35]	95.86 [88.57]	86.16 [81.14]	86.72 [81.34]
Salmonella phage vB_SalM_PC127	91.94 [82.76]	87.39 [79.43]	90.94 [69.92]	88.35 [73.08]	87.05 [74.35]	85.72 [79.38]	85.84 [81.54]	-	85.74 [79.31]	99.96 [97.96]	91.09 [79.41]
Salmonella phage vB_SalM- LPST153	85.72 [84.58]	93.67 [88.30]	87.79 [77.39]	86.71 [76.30]	91.35 [91.04]	99.98 [97.86]	96.42 [88.85]	86.77 [79.92]	-	86.88 [79.81]	87.20 [77.22]
Salmonella phage vB_SalS_PC192	91.70 [89.43]	87.27 [83.04]	90.14 [78.61]	88.26 [77.75]	88.27 [78.64]	86.37 [83.22]	86.26 [82.50]	99.97 [95.91]	86.38 [82.65]	-	90.85 [86.30]
Salmonella phage vB_STy-RN5i1	91.84 [85.73]	87.31 [80.43]	91.35 [75.17]	89.44 [73.66]	88.43 [70.11]	87.10 [75.84]	87.16 [80.68]	91.14 [82.36]	87.11 [75.80]	91.27 [81.86]	-

3.1.4. Host Range Analysis

Salmonella phage SPYS_1 is able to infect and form plaques on 5 out of 13 *Salmonella* strains, including four *S. typhimurium* strains and one *Salmonella choleraesuis* (Figure 3). In comparison, *Salmonella* phage SPYS_2 showed a similar but broader host range (Figure 3). *Salmonella* phage SPYS_2 can not only form plaques on all strains sensitive to phage SPYS_1 but is also on *Salmonella Typhi* (CICC10871) and *Salmonella Paratyphi B* (CICC10437).

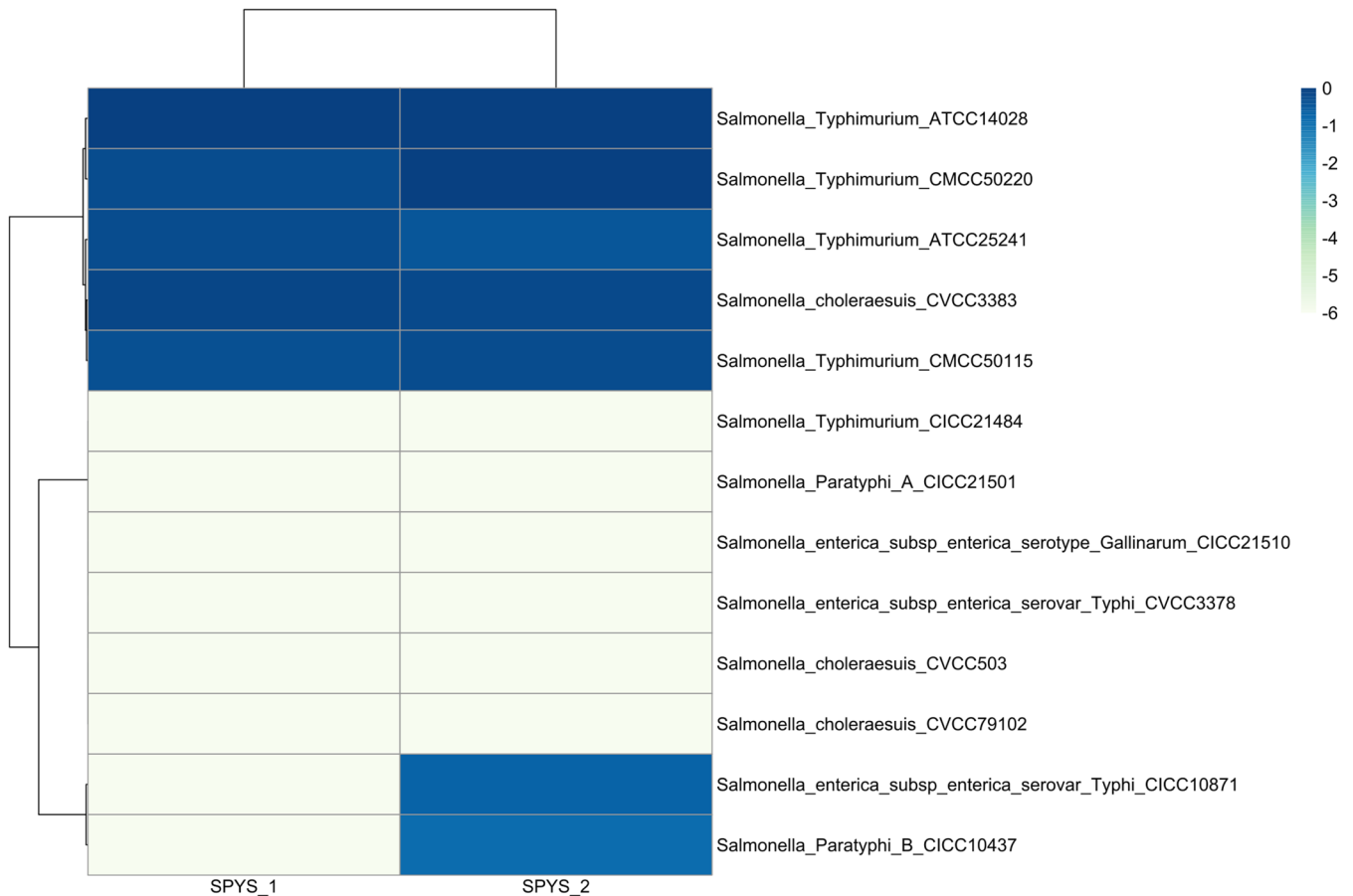


Figure 3. Efficiencies of plating results of two *Salmonella* phages against standard strains of *Salmonella* with different serotypes. The EOP for each phage on each strain represented the relative value of the titer compared to the highest titer of that specific phage across all strains. The values are the average of three biological replicates.

Interestingly, despite distinct morphologies and genomes, SPYS_1 and SPYS_2 share a similar host range (Figure 3). Among thirteen *Salmonella* strains, five are sensitive to both SPYS_1 and SPYS_2, while six show resistance to both phages. SPYS_1 and SPYS_2 only displayed different performances on *S. Typhi* (CICC10871) and *S. Paratyphi B* (CICC10437) (Figure 3).

3.1.5. Phage SPYS_1 and SPYS_2 Stability

Chloroform is a crucial agent utilized in experiments such as liquid amplification and the one-step growth curve. Phages with capsids containing lipid components are sensitive to chloroform, leading to a significant reduction in titers following treatment [39]. The chloroform stability test revealed that the titers of phage SPYS_1 and SPYS_2 were not affected by chloroform (Table S1).

Thermal stress stability tests demonstrated that phage SPYS_1 exhibited high stability within the temperature range of 4–70 °C for 1 h but was entirely inactivated at 80 °C (Figure 4A). In comparison, phage SPYS_2 displayed reduced stability under thermal stress,

with a 5-log reduction observed at 60 °C, and it was completely inactivated at temperatures exceeding 70 °C (Figure 4B).

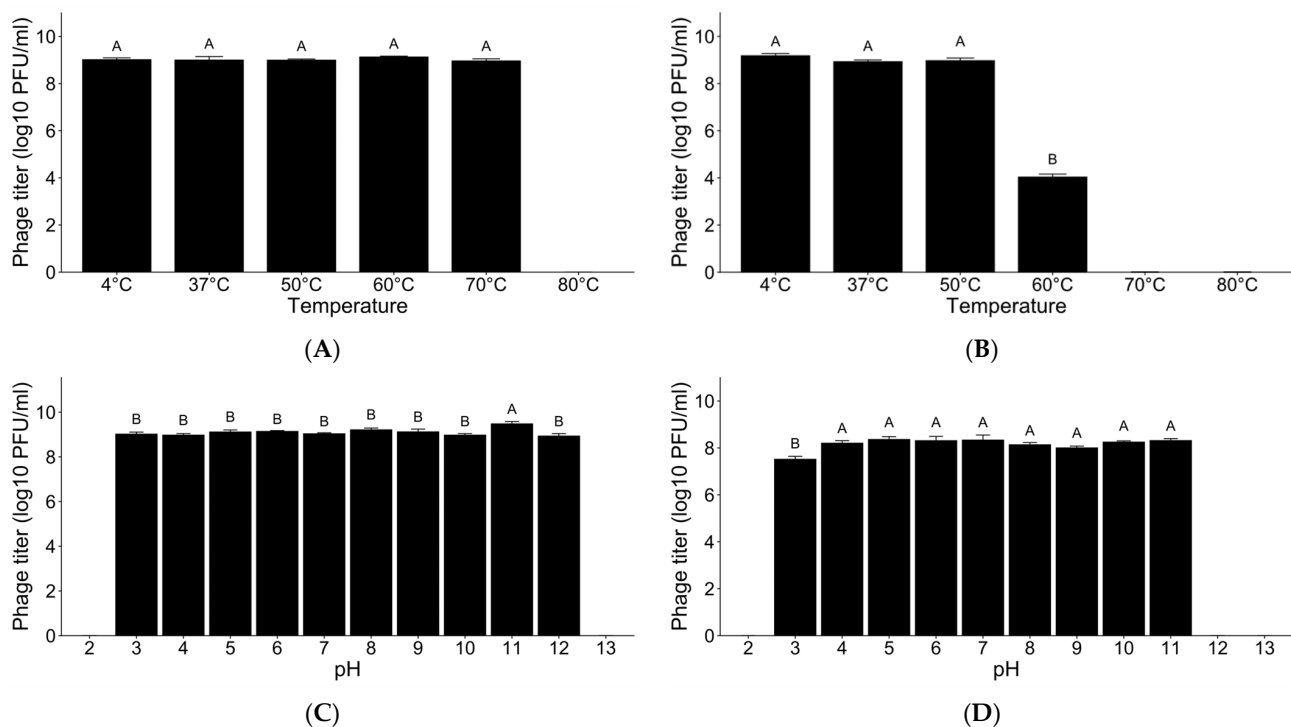


Figure 4. The thermal and pH stress stability of two *Salmonella* phages. (A) *Salmonella* phage SPYS_1 stability against thermal stress; (B) *Salmonella* phage SPYS_2 stability against thermal stress; (C) *Salmonella* phage SPYS_1 stability against pH stress; (D) *Salmonella* phage SPYS_2 stability against pH stress. The values are the average of three biological replicates, error bars represent standard errors. The Student–Newman–Keuls test was employed in each experiment, and different capital letters represent significant differences ($p < 0.05$) among experiment groups.

pH stress stability tests revealed that phages SPYS_1 and SPYS_2 showed remarkable stability within a pH range of 3–11 for 24 h but were inactivated when pH levels dropped to 2 or rose to 13 (Figure 4C,D).

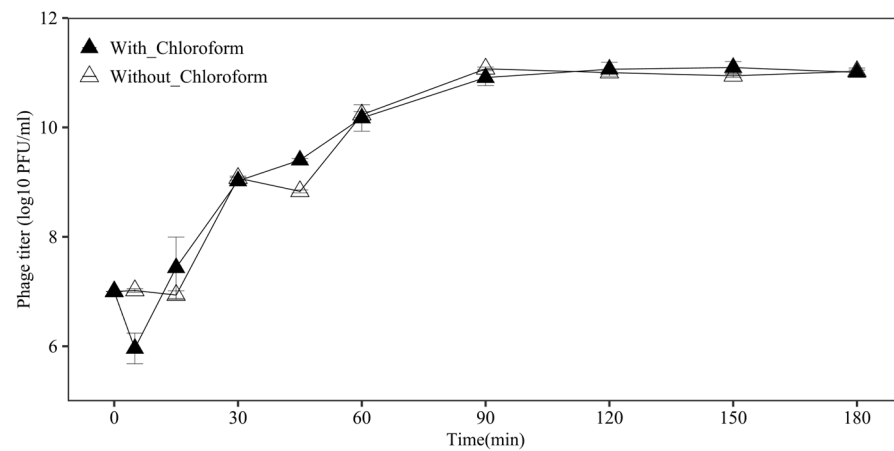
3.2. Growth Characteristics of *Salmonella* Phages

3.2.1. One-Step Growth Curve Experiment

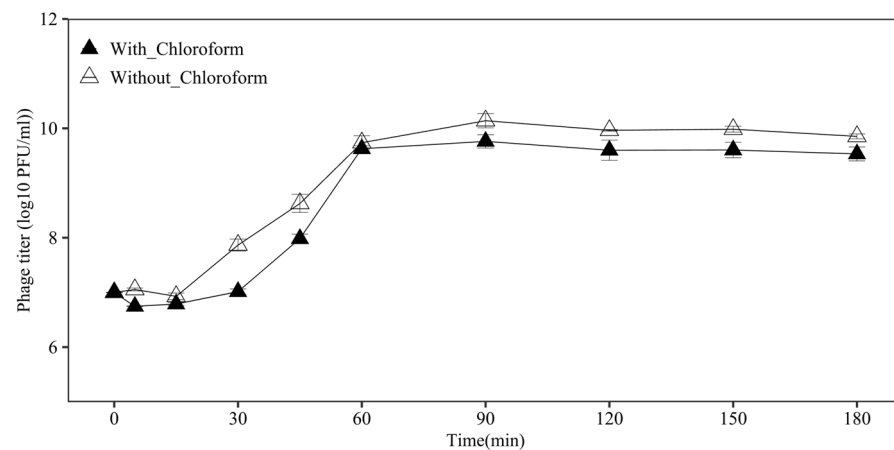
Salmonella phage SPYS_1 was found to share a similar adsorption time but a higher adsorption rate than *Salmonella* phage SPYS_2 (Figure 5A,B). At 5 min post-infection, the adsorption rate of phage SPYS_1 was 86.80% (7.17% standard deviation), while only 41% (2.52% standard deviation) of phage SPYS_2 had absorbed *S. typhimurium* ATCC 14028.

Interestingly, the phage SPYS_1 likely experienced two complete lytic cycles within 90 min, completing the first lytic cycle in 30 min, initiating the second round of adsorption at 30–45 min, and finishing the second lytic cycle at 30–90 min. In the first lytic cycle, the phage SPYS_1 showed a latent period of 15–30 min, an eclipse period of 5–15 min, and a burst size of ~119.0 (SE, 9.8) PFU/cell (Figure 5A). The analysis of the second lytic cycle showed a latent period of 15–30 min and a burst size of ~100.0 (SE, 6.8) PFU/cell (Figure 5A). Although the second lytic cycle of the phage SPYS_1 showed similar infection kinetics, the total cycle consumed double the time compared to the first cycle (Figure 5A). One probable explanation is the uninfected cell needs time to propagate, providing enough host strain for phage binding in the second cycle. The phage SPYS_2 can complete one lytic cycle with an MOI of 0.1 in 60 min, showing a latent period of 15–30 min, an eclipse period of 5–15 min, and a burst size of ~1516.7 (SE, 492.7) PFU/cell (Figure 5B). Although

the phage SPYS_2 has a much higher burst size, the final concentration was ~1 log lower than the phage SYSP_1 in the one-step growth curve experiment due to the occurrence of a second lytic cycle (Figure 5A,B).



(A)

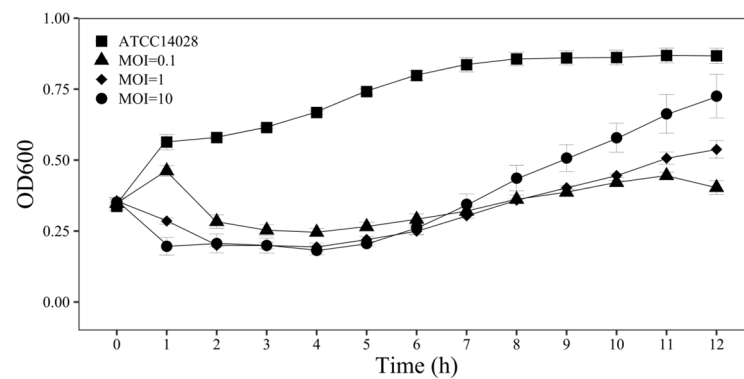


(B)

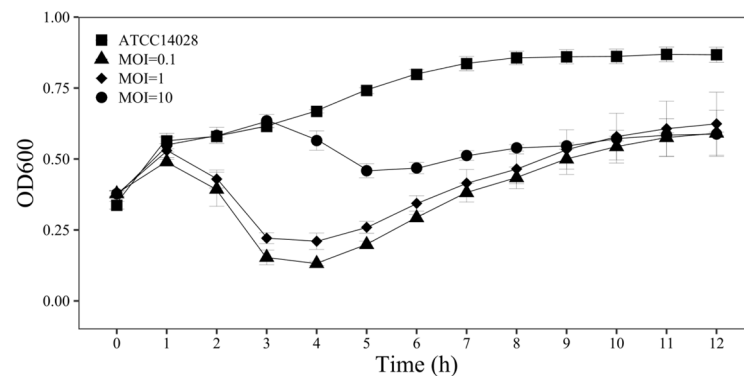
Figure 5. One-step growth curve of *S. typhimurium* ATCC 14028 treated with (A) *Salmonella* phage SPYS_1 and (B) *Salmonella* phage SPYS_2 at an MOI of 0.1 at 37 °C. Filled triangles represent the phage samples treated with chloroform and unfilled triangles represent the phage samples treated without chloroform. The values are the average of three biological replicates; error bars represent standard errors.

3.2.2. Growth Inhibition Experiment

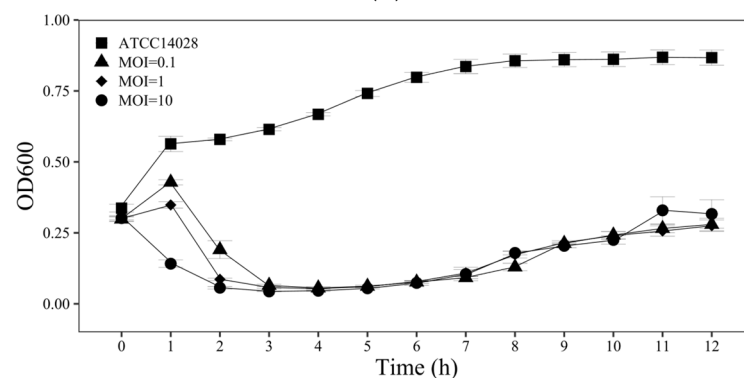
The growth of *S. typhimurium* ATCC 14028 was inhibited by the phage SPYS_1 at different dosages (Figure 6A). The results suggested that the OD_{600nm} of *S. typhimurium* ATCC 14028 decreased from ~0.35 to ~0.19 in the first four hours, and the re-growth was observed after being treated with higher phage dosages (MOI = 1 or 10), maintaining OD_{600nm} under 0.3 for 6 h. When treated with a low dosage (MOI = 0.1), the growth of *S. typhimurium* ATCC 14028 increased in the first hour, which was followed by a decrease over the next three hours. Re-growth was observed after 4 h, maintaining OD_{600nm} under 0.3 between 2 h and 6 h. Although a higher phage dosage of SPYS_1 treatment could inhibit the growth of the host strain to a lower OD_{600nm} in 6 h, the final concentration of strain treated with different dosages of SPYS_1 showed an opposite trend (Figure 6A). One possible explanation is that the emergence and re-growth of the resistant strains were accelerated when treated with a high phage dosage, leading to lower phage production levels during later infection (Figure 6A).



(A)



(B)



(C)

Figure 6. Inhibition growth curve of *S. typhimurium* ATCC 14028 treated with (A) *Salmonella* phage SPYS_1, (B) *Salmonella* phage SPYS_2, or (C) a mixture of phages at different MOIs. Filled squares represent the samples treated with SM buffer, filled triangles represent samples treated at an MOI of 0.1, filled diamonds represent samples treated at an MOI of 1, filled circles represent samples treated at an MOI of 10. The values are the average of three biological replicates, error bars represent standard errors.

The phage SPYS_2 also showed an inhibition effect on the growth of *S. typhimurium* ATCC at different dosages (Figure 6B). When treated with low dosages, phage SPYS_2 showed high efficiency in inhibiting the growth of the host strain, keeping OD_{600nm} of *S. typhimurium* ATCC 14028 under 0.3 between 3 h and 6 h with MOI = 0.1, and between 3 h and 5 h with MOI = 1 (Figure 6B).

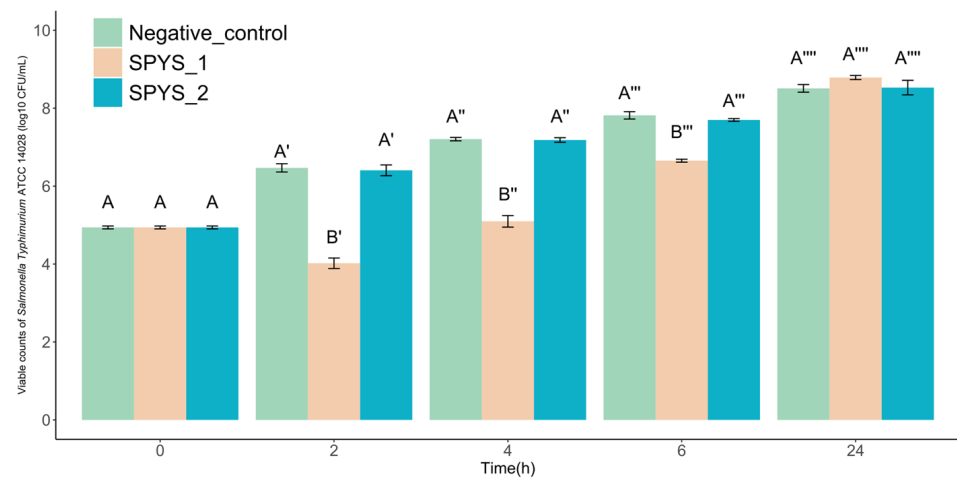
The phage cocktail, combining equivalent amounts of SPYS_1 and SPYS_2, demonstrated high efficiency in inhibiting the growth of *S. typhimurium* ATCC 14028 (Figure 6C). Even at a low dosage (MOI = 0.1), the combined phage stock maintained OD_{600nm} under 0.3 for at least 12 h (Figure 6C). The emergence and re-growth of the resistant strains were

reduced by the cocktail, suggesting the combination of different phage types could be an effective solution to phage-resistant mechanisms.

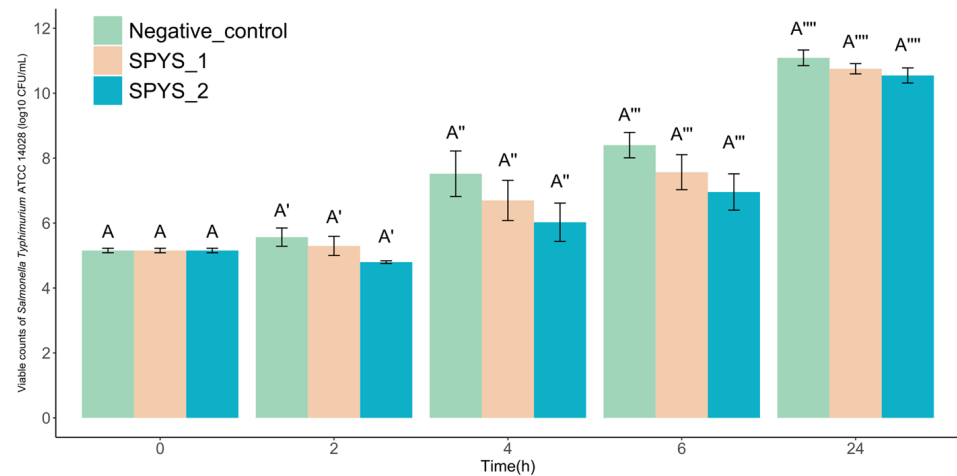
3.3. Food Applications of Salmonella Phages

3.3.1. The Biocontrol Effect of Salmonella Phages in Milk

The phage SPYS_1 showed a significant antibacterial effect on the growth of *S. typhimurium* ATCC 14028 in milk when treated at 37 °C and MOI = 0.1 at a range of 2 to 6 h ($p < 0.05$) (Figure 7A). The concentration of viable bacteria in milk showed a ~2-log reduction for 2 h and 4 h and a ~1-log reduction for 6 h when treated with phage SPYS_1 compared to the control group that was treated with SM buffer. However, the phage SPYS_2 appeared to have no influence on the growth of *S. typhimurium* ATCC 14028 when treated at 37 °C and MOI = 0.1, suggesting the phage SPYS_2 may not be able to adapt to the environment of milk.



(A)



(B)

Figure 7. The biocontrol effect of *Salmonella* phage SPYS_1 and SPYS_2 against *Salmonella typhimurium* ATCC 14028 on (A) milk and (B) chicken tenders at an MOI of 0.1. Light green represents the samples treated with SM buffer, light pink represents the samples treated with *Salmonella* phage SPYS_1, and light blue represents the samples treated with *Salmonella* phage SPYS_2. The values are the average of three biological replicates, error bars represent standard errors. The Student–Newman–Keuls test was employed at each time point, and different capital letters represent significant differences ($p < 0.05$) among experiment groups.

3.3.2. The Biocontrol Effect of Salmonella Phage in Chicken Tender

Both phage SPYS_1 and phage SPYS_2 have no significant antibacterial effect on the growth of *S. typhimurium* ATCC 14028 on chicken tenders when treated at 37 °C and MOI = 0.1 ($p > 0.05$) (Figure 7B). However, the phage SPYS_2 had a better performance in inhibiting the growth of the viable bacteria on the surface of the chicken, showing a ~1-log reduction at 2 h, 4 h, and 6 h compared to the phage SPYS_1 (Figure 7B). Considering the low adsorption rate in liquid media and weak inhibition effect in milk on the host strain, the phage SPYS_2 may be more suitable to be applied in solid environments, which requires more evidence and experiments to confirm.

4. Discussion

S. typhimurium is a major cause of foodborne gastroenteritis [40]. The overuse and misuse of antibiotics exacerbate global health risks, leading to stringent regulations on antibiotic residues in food [41]. As eco-friendly antibacterial agents, bacteriophages offer a promising alternative for controlling *Salmonella* contamination without compromising food quality [15,42]. To date, several commercial phage products have been developed to control *Salmonella* in foods and animal feed, such as SalmoShield, SalmoLyse, SalmoFresh, and BioTector [42]. However, the antibacterial effect of phage may be weakened or even invalidated due to the emergence of the mutant strains that resist phage infection [24,43]. The most effective solution currently is to use a phage cocktail, which reduces the likelihood of resistant strains emerging [44]. Therefore, there is an urgent need for novel phages with strong lytic capabilities for phage biocontrol technology in the food industry [45]. In this study, we isolated and characterized two novel *Salmonella* phages and evaluated their biocontrol effectiveness on milk and chicken tenders. The results showed that the isolated phages have the necessary characteristics for food safety applications, though some challenges remain.

The type of phage replication cycle is a key factor that determines its potential applications for food safety. Based on their replication cycles, bacteriophages can be classified into lytic phages and temperate phages [46]. Temperate phages are known to be involved in horizontal gene transfer, increasing the pathogenicity and fitness of pathogens [47]. Therefore, only strictly lytic phages are allowed to be used for application purposes in the food industry due to safety concerns [48]. Genome analysis has predicted that *Salmonella* phages SPYS_1 and SPYS_2 are lytic phages with no virulence genes, making them ideal candidates for the biocontrol of pathogens in the food industry.

The stability of phages is another crucial factor in determining their suitability as antibacterial agents in food [49]. Since the actual application environment is more complex than laboratory conditions, various factors can influence the effectiveness of phage treatments with temperature and pH being primary environmental limitations [49,50]. For instance, the *E. coli* Stx phage remained stable in tap water (pH 7.4) or semi-skimmed milk (pH 6.7) at room temperature but was completely inactivated in orange juice (pH 3.9) after 24 h [51]. The pH of poultry meat ranges from 5.2 to 7.0, while milk has a pH between 6.5 and 6.7 [52,53]. Both products are typically stored at 4 °C. In this study, *Salmonella* phages SPYS_1 and SPYS_2 showed excellent tolerance to a broad range of temperatures and pH levels, suggesting they are strong candidates for biocontrol of *S. typhimurium* in milk and chicken tenders.

Phage replication kinetics are essential for predicting population dynamics, which is critical for optimizing phage applications. The one-step growth curve is fundamental for understanding the phage lysis cycle, indicating the adsorption rate, latent period, eclipse period, and burst size [54]. Notably, only 41% of phage SPYS_2 adsorbed to *S. typhimurium* ATCC 14028, which was much lower than the adsorption rate of phage SPYS_1. We propose that *S. typhimurium* ATCC 14028 likely possesses a resistance mechanism that inhibits the adsorption of phage SPYS_2, thus limiting the propagation efficiency of phage SPYS_2. The phage adsorption capacity may be improved by co-culturing the phage SPYS_1 with *S. typhimurium* ATCC 14028 and isolating the mutant phages that overcome the resistance

mechanism [37]. The one-step growth curve results demonstrated that both isolated phages could proliferate rapidly under suitable conditions, making them suitable for industrial production.

However, the emergence of phage-resistant mutants is still the main challenge to the phage application. The host strain can easily develop phage-resistant mutants under the selective pressure of phage treatment [55]. Resistant mutants can prevent phage infection through various mechanisms, including adsorption inhibition, degradation of phage DNA, and abortive infection [56,57]. In growth inhibition experiments, the re-growth of phage-resistant mutants was observed within five hours when treated with a single phage. However, the emergence of re-growth was delayed when treated with a combination of phages SPYS_1 and SPYS_2. One possible explanation is that mutant strains adopt different resistance mechanisms when treated with SPYS_1 and SPYS_2, making it significantly more difficult to develop mutants resistant to both phages. Moreover, the growth rate of the re-growth also slowed down. The emergence of phage resistance is often accompanied by a reduction in bacterial fitness [58]. Therefore, we propose that more fitness must be sacrificed for survival when treated with a combination of different phages, suggesting that phage cocktails could be an effective solution to phage resistance.

Phage cocktails are currently the primary strategy to overcome phage resistance. Although cocktail treatment showed improved inhibition of host strain growth, phages SPYS_1 and SPYS_2 have a similar host range, which was likely due to their isolation from the same environment. For a phage cocktail to be effective in treating *Salmonella* contamination in food, its host range must cover the most common and pathogenic serotypes. Therefore, while SPYS_1 and SPYS_2 can be part of a phage cocktail, additional phages with complementary host ranges are necessary. Consequently, the isolation of novel lytic phages remains a crucial task for the effective application of phages in food safety.

Endolysins represent another viable strategy for overcoming phage resistance. At the end of the lytic cycle, bacteriophages encode endolysins that target the conserved structure of the peptidoglycan layer, effectively cleaving bacteria and biofilms [59]. As an antibacterial protein encoded by phages, endolysin not only inherits the advantages of phage efficiency and safety but also presents no risk of developing mutant strains, according to current research [60,61]. The endolysin-encoded genes of phage SPYS_1 and SPYS_2 were annotated in the genome maps (Figure 2A,B). With the known sequences, the endolysins could be expressed via heterologous expression technology, offering another strategy for the biocontrol of pathogens in food [61].

The complexity of the environment and food composition are key factors limiting the effectiveness of phage biocontrol in food. In the study, the biocontrol effect of phages SPYS_1 and SPYS_2 against *S. typhimurium* ATCC 14028 on milk and chicken tenders is not as effective as expected, which is possibly due to food ingredients influencing the activity and efficacy of phages [50]. For instance, raw milk was found to protect *S. aureus* from phage adsorption by sterically blocking the attachment sites with whey proteins [62]. Since phages SPYS_1 and SPYS_2 showed a significant inhibition of *S. typhimurium* ATCC 14028 in BHI media, a suitable encapsulation strategy or delivery system is required to shield phages from the influence of food ingredients and ensure their delivery to targets [50].

Above all, *Salmonella* phages SPYS_1 and SPYS_2 have shown significant potential for biocontrolling *Salmonella* in food. However, directly adding phages has demonstrated a poor antibacterial effect due to the interaction of food components with phage activity. Overcoming the impact of food on phage efficacy remains a critical challenge for their application.

5. Conclusions

In this study, we isolated, purified, and characterized two lytic *Salmonella* phages against *S. typhimurium* ATCC 14028, the phage SPYS_1 and the phage SPYS_2. Based on the morphology characteristic and genome analysis, *Salmonella* phage SPYS_1 was identified as a novel species belonging to the genus *Skatevirus*, while *Salmonella* phage SPYS_2 is

identified as a novel species belongs to the *genus Berlinvirus*. Both phages exhibited high stabilities under the conditions of chloroform treatment, thermal stress, and pH stress. The phage SPYS_1 exhibited a high antibacterial activity in a liquid environment, and the addition of the phage SPYS_2 can reduce the emergence of the resistant mutants, suggesting these phages could be good candidates to reduce *S. typhimurium* contamination in milk and poultry meat products.

Supplementary Materials: The following supporting information can be downloaded at: <https://www.mdpi.com/article/10.3390/foods13193103/s1>, Table S1. The chloroform sensitivity of phage SPYS_1 and SPYS_2. Figure S1. Efficiencies of plaquing results of two *Salmonella* phages against standard strains of *Salmonella* with different stereotypes. The EOP for each phage on each strain represented the relative value of the titer compared to the highest titer of that specific phage across all strains.

Author Contributions: Conceptualization, Y.S. (Yaxiong Song), Y.H., B.Z. and J.W.; Methodology, Y.S. (Yaxiong Song), Y.H., B.Z., J.W., Y.S. (Yi Sun) and W.F.; Formal analysis, W.G., X.L. and X.X.; Investigation, Y.S. (Yaxiong Song); Writing—original draft, Y.S. (Yaxiong Song); Writing—review & editing, Y.S. (Yaxiong Song), W.G., Y.H., B.Z., Y.S. (Yi Sun) and W.F.; Visualization, Y.S. (Yaxiong Song), X.L. and X.X.; Supervision, S.W.; Funding acquisition, Y.S. (Yaxiong Song), J.W. and S.W. All authors have read and agreed to the published version of the manuscript.

Funding: This research was funded by “the Fundamental Research Funds for the Central Universities”, Nankai University (Grant Number 730-63241461) and National Key Research and Development Program of China (Grant Number 2022YFF1100704).

Institutional Review Board Statement: Not applicable.

Informed Consent Statement: Not applicable.

Data Availability Statement: The original contributions presented in the study are included in the article/Supplementary Material, further inquiries can be directed to the corresponding author.

Conflicts of Interest: The authors declare no conflict of interest.

References

- Romero-Calle, D.X.; Pedrosa-Silva, F.; Ribeiro Tomé, L.M.; Fonseca, V.; Guimarães Benevides, R.; de Oliveira Santos, L.T.S.; de Oliveira, T.; da Costa, M.M.; Alcantara, L.C.J.; de Carvalho Azevedo, V.A. Molecular Characterization of *Salmonella* Phage Wara Isolated from River Water in Brazil. *Microorganisms* **2023**, *11*, 1837. [\[CrossRef\]](#) [\[PubMed\]](#)
- Ehuwa, O.; Jaiswal, A.K.; Jaiswal, S. *Salmonella*, food safety and food handling practices. *Foods* **2021**, *10*, 907. [\[CrossRef\]](#) [\[PubMed\]](#)
- Mohammed, M.; Casjens, S.R.; Millard, A.D.; Harrison, C.; Gannon, L.; Chattaway, M.A. Genomic analysis of Anderson typing phages of *Salmonella typhimurium*: Towards understanding the basis of bacteria-phage interaction. *Sci. Rep.* **2023**, *13*, 10484. [\[CrossRef\]](#) [\[PubMed\]](#)
- Ruvalcaba-Gómez, J.M.; Villagrán, Z.; Valdez-Alarcón, J.J.; Martínez-Núñez, M.; Gomez-Godínez, L.J.; Ruesga-Gutiérrez, E.; Anaya-Esparza, L.M.; Arteaga-Garibay, R.I.; Villarruel-López, A. Non-antibiotics strategies to control *Salmonella* infection in poultry. *Animals* **2022**, *12*, 102. [\[CrossRef\]](#) [\[PubMed\]](#)
- Yan, T.; Liang, L.; Yin, P.; Zhou, Y.; Mahdy Sharoba, A.; Lu, Q.; Dong, X.; Liu, K.; Connerton, I.F.; Li, J. Application of a novel phage LPSEYT for biological control of *Salmonella* in foods. *Microorganisms* **2020**, *8*, 400. [\[CrossRef\]](#)
- Zhang, Y.; Ding, Y.; Li, W.; Zhu, W.; Wang, J.; Wang, X. Application of a novel lytic podoviridae phage Pu20 for biological control of drug-resistant *Salmonella* in liquid eggs. *Pathogens* **2021**, *10*, 34. [\[CrossRef\]](#) [\[PubMed\]](#)
- Wang, X.; Biswas, S.; Paudyal, N.; Pan, H.; Li, X.; Fang, W.; Yue, M. Antibiotic resistance in *Salmonella typhimurium* isolates recovered from the food chain through national antimicrobial resistance monitoring system between 1996 and 2016. *Front. Microbiol.* **2019**, *10*, 985. [\[CrossRef\]](#)
- Galán, J.E. *Salmonella typhimurium* and inflammation: A pathogen-centric affair. *Nat. Rev. Microbiol.* **2021**, *19*, 716–725. [\[CrossRef\]](#)
- Park, H.; Kim, J.; Kim, H.; Cho, E.; Park, H.; Jeon, B.; Ryu, S. Characterization of the lytic phage MSP1 for the inhibition of multidrug-resistant *Salmonella enterica* serovars Thompson and its biofilm. *Int. J. Food Microbiol.* **2023**, *385*, 110010. [\[CrossRef\]](#)
- Roasto, M.; Bonardi, S.; Mäesaar, M.; Alban, L.; Gomes-Neves, E.; Vieira-Pinto, M.; Vågsholm, I.; Elias, T.; Lindegaard, L.L.; Blagojevic, B. *Salmonella enterica* prevalence, serotype diversity, antimicrobial resistance and control in the European pork production chain. *Trends Food Sci. Technol.* **2023**, *131*, 210–219. [\[CrossRef\]](#)
- Majowicz, S.E.; Musto, J.; Scallan, E.; Angulo, F.J.; Kirk, M.; O'Brien, S.J.; Jones, T.F.; Fazil, A.; Hoekstra, R.M.; Studies, I.C.o.E.D.B.o.I. The global burden of nontyphoidal *Salmonella* gastroenteritis. *Clin. Infect. Dis.* **2010**, *50*, 882–889. [\[CrossRef\]](#) [\[PubMed\]](#)

12. Islam, M.S.; Hu, Y.; Mizan, M.F.R.; Yan, T.; Nime, I.; Zhou, Y.; Li, J. Characterization of *Salmonella* phage LPST153 that effectively targets most prevalent *Salmonella* serovars. *Microorganisms* **2020**, *8*, 1089. [CrossRef]
13. Hoffmann, S.; Batz, M.B.; Morris, J.G., Jr. Annual cost of illness and quality-adjusted life year losses in the United States due to 14 foodborne pathogens. *J. Food Prot.* **2012**, *75*, 1292–1302. [CrossRef] [PubMed]
14. Economic Research Service. Department of Agriculture (USDA). 2021. Available online: <https://www.ers.usda.gov/data-products/cost-estimates-of-foodborne-illnesses.aspx> (accessed on 22 March 2024).
15. Cao, Y.; Ma, R.; Li, Z.; Mao, X.; Li, Y.; Wu, Y.; Wang, L.; Han, K.; Li, L.; Ma, D. Broad-Spectrum *Salmonella* Phages PSE-D1 and PST-H1 Controls *Salmonella* in Foods. *Viruses* **2022**, *14*, 2647. [CrossRef] [PubMed]
16. Shang, Y.; Sun, Q.; Chen, H.; Wu, Q.; Chen, M.; Yang, S.; Du, M.; Zha, F.; Ye, Q.; Zhang, J. Isolation and characterization of a novel *Salmonella* phage vB_SalP_TR2. *Front. Microbiol.* **2021**, *12*, 664810. [CrossRef] [PubMed]
17. Sukjoi, C.; Buddhasiri, S.; Tantibhadrasapa, A.; Kaewsakhorn, T.; Phothaworn, P.; Nale, J.Y.; Lopez-Garcia, A.V.; AbuOun, M.; Anjum, M.F.; Malik, D.J. Therapeutic effects of oral administration of lytic *Salmonella* phages in a mouse model of non-typhoidal salmonellosis. *Front. Microbiol.* **2022**, *13*, 955136. [CrossRef] [PubMed]
18. Bai, J.; Jeon, B.; Ryu, S. Effective inhibition of *Salmonella Typhimurium* in fresh produce by a phage cocktail targeting multiple host receptors. *Food Microbiol.* **2019**, *77*, 52–60. [CrossRef] [PubMed]
19. Huang, C.; Shi, J.; Ma, W.; Li, Z.; Wang, J.; Li, J.; Wang, X. Isolation, characterization, and application of a novel specific *Salmonella* bacteriophage in different food matrices. *Food Res. Int.* **2018**, *111*, 631–641. [CrossRef] [PubMed]
20. Li, C.; Wang, Y.; Wang, J.; Wang, X. Properties of a Novel *Salmonella* Phage L66 and Its Application Based on Electrochemical Sensor-Combined AuNPs to Detect *Salmonella*. *Foods* **2022**, *11*, 2836. [CrossRef]
21. Perera, M.N.; Abuladze, T.; Li, M.; Woolston, J.; Sulakvelidze, A. Bacteriophage cocktail significantly reduces or eliminates *Listeria monocytogenes* contamination on lettuce, apples, cheese, smoked salmon and frozen foods. *Food Microbiol.* **2015**, *52*, 42–48. [CrossRef]
22. Moye, Z.; Woolston, J.; Sulakvelidze, A. Bacteriophage applications for food production and processing. *Viruses* **2018**, *10*, 205. [CrossRef] [PubMed]
23. Pires, D.P.; Costa, A.R.; Pinto, G.; Meneses, L.; Azeredo, J. Current challenges and future opportunities of phage therapy. *FEMS Microbiol. Rev.* **2020**, *44*, 684–700. [CrossRef] [PubMed]
24. Song, Y.; Peters, T.L.; Bryan, D.W.; Hudson, L.K.; Denes, T.G. Characterization of a Novel Group of *Listeria* Phages That Target Serotype 4b *Listeria monocytogenes*. *Viruses* **2021**, *13*, 671. [CrossRef]
25. Guo, Y.; Li, J.; Islam, M.S.; Yan, T.; Zhou, Y.; Liang, L.; Connerton, I.F.; Deng, K.; Li, J. Application of a novel phage vB_SalS-LPSTLL for the biological control of *Salmonella* in foods. *Food Res. Int.* **2021**, *147*, 110492. [CrossRef] [PubMed]
26. Chen, Y.; Chen, Y.; Shi, C.; Huang, Z.; Zhang, Y.; Li, S.; Li, Y.; Ye, J.; Yu, C.; Li, Z. SOAPnuke: A MapReduce acceleration-supported software for integrated quality control and preprocessing of high-throughput sequencing data. *Gigascience* **2018**, *7*, gix120. [CrossRef]
27. Li, H.; Durbin, R. Fast and accurate short read alignment with Burrows–Wheeler transform. *Bioinformatics* **2009**, *25*, 1754–1760. [CrossRef] [PubMed]
28. Li, D.; Luo, R.; Liu, C.-M.; Leung, C.-M.; Ting, H.-F.; Sadakane, K.; Yamashita, H.; Lam, T.-W. MEGAHIT v1.0: A fast and scalable metagenome assembler driven by advanced methodologies and community practices. *Methods* **2016**, *102*, 3–11. [CrossRef]
29. Nayfach, S.; Camargo, A.P.; Schulz, F.; Elie-Fadrosh, E.; Roux, S.; Kyrpides, N.C. CheckV assesses the quality and completeness of metagenome-assembled viral genomes. *Nat. Biotechnol.* **2021**, *39*, 578–585. [CrossRef] [PubMed]
30. Mihara, T.; Nishimura, Y.; Shimizu, Y.; Nishiyama, H.; Yoshikawa, G.; Uehara, H.; Hingamp, P.; Goto, S.; Ogata, H. Linking virus genomes with host taxonomy. *Viruses* **2016**, *8*, 66. [CrossRef] [PubMed]
31. Shang, J.; Tang, X.; Sun, Y. PhaTYP: Predicting the lifestyle for bacteriophages using BERT. *Brief. Bioinform.* **2023**, *24*, bbac487. [CrossRef] [PubMed]
32. Richter, M.; Rosselló-Móra, R.; Oliver Glöckner, F.; Peplies, J. JSpeciesWS: A web server for prokaryotic species circumscription based on pairwise genome comparison. *Bioinformatics* **2016**, *32*, 929–931. [CrossRef]
33. Kurtz, S.; Phillippy, A.; Delcher, A.L.; Smoot, M.; Shumway, M.; Antonescu, C.; Salzberg, S.L. Versatile and open software for comparing large genomes. *Genome Biol.* **2004**, *5*, R12. [CrossRef]
34. Richter, M.; Rosselló-Móra, R. Shifting the genomic gold standard for the prokaryotic species definition. *Proc. Natl. Acad. Sci. USA* **2009**, *106*, 19126–19131. [CrossRef]
35. Brettin, T.; Davis, J.J.; Disz, T.; Edwards, R.A.; Gerdes, S.; Olsen, G.J.; Olson, R.; Overbeek, R.; Parrello, B.; Pusch, G.D. RASTtk: A modular and extensible implementation of the RAST algorithm for building custom annotation pipelines and annotating batches of genomes. *Sci. Rep.* **2015**, *5*, 8365. [CrossRef] [PubMed]
36. Grant, J.R.; Enns, E.; Marinier, E.; Mandal, A.; Herman, E.K.; Chen, C.-y.; Graham, M.; Van Domselaar, G.; Stothard, P. Proksee: In-depth characterization and visualization of bacterial genomes. *Nucleic Acids Res.* **2023**, *51*, W484–W492. [CrossRef]
37. Peters, T.L.; Song, Y.; Bryan, D.W.; Hudson, L.K.; Denes, T.G. Mutant and recombinant phages selected from in vitro coevolution conditions overcome phage-resistant *Listeria monocytogenes*. *Appl. Environ. Microbiol.* **2020**, *86*, e02138-20. [CrossRef]
38. Kolde, R. Pheatmap: Pretty Heatmaps (Version 1.0.12). 2019. Available online: <https://rdrr.io/cran/pheatmap/> (accessed on 22 March 2024).

39. Xiang, Y.; Li, W.; Song, F.; Yang, X.; Zhou, J.; Yu, H.; Ji, X.; Wei, Y. Biological characteristics and whole-genome analysis of the *Enterococcus faecalis* phage PEf771. *Can. J. Microbiol.* **2020**, *66*, 505–520. [[CrossRef](#)]
40. Zhu, H.; Sydor, A.M.; Boddy, K.C.; Coyaud, E.; Laurent, E.M.; Au, A.; Tan, J.M.; Yan, B.-R.; Moffat, J.; Muise, A.M. *Salmonella* exploits membrane reservoirs for invasion of host cells. *Nat. Commun.* **2024**, *15*, 3120. [[CrossRef](#)]
41. Redwan Haque, A.; Sarker, M.; Das, R.; Azad, M.A.K.; Hasan, M.M. A review on antibiotic residue in foodstuffs from animal source: Global health risk and alternatives. *Int. J. Environ. Anal. Chem.* **2023**, *103*, 3704–3721. [[CrossRef](#)]
42. Oh, J.-H.; Park, M.-K. Recent trends in *Salmonella* outbreaks and emerging technology for biocontrol of *Salmonella* using phages in foods: A review. *J. Microbiol. Biotechnol.* **2017**, *27*, 2075–2088. [[CrossRef](#)]
43. Song, Y.; Peters, T.L.; Bryan, D.W.; Hudson, L.K.; Denes, T.G. *Homburgvirus* LP-018 Has a Unique Ability to Infect Phage-Resistant *Listeria monocytogenes*. *Viruses* **2019**, *11*, 1166. [[CrossRef](#)]
44. Ribeiro, J.M.; Pereira, G.N.; Durli Junior, I.; Teixeira, G.M.; Bertozzi, M.M.; Verri, W.A., Jr.; Kobayashi, R.K.T.; Nakazato, G. Comparative analysis of effectiveness for phage cocktail development against multiple *Salmonella* serovars and its biofilm control activity. *Sci. Rep.* **2023**, *13*, 13054. [[CrossRef](#)]
45. Zalewska-Piątek, B. Phage therapy—Challenges, opportunities and future prospects. *Pharmaceuticals* **2023**, *16*, 1638. [[CrossRef](#)]
46. Dennehy, J.J.; Abedon, S.T. Phage infection and lysis. In *Bacteriophages: Biology, Technology, Therapy*; Springer: Berlin/Heidelberg, Germany, 2021; pp. 341–383.
47. Gummalla, V.S.; Zhang, Y.; Liao, Y.-T.; Wu, V.C. The role of temperate phages in bacterial pathogenicity. *Microorganisms* **2023**, *11*, 541. [[CrossRef](#)] [[PubMed](#)]
48. Hibstu, Z.; Belew, H.; Akelew, Y.; Mengist, H.M. Phage therapy: A different approach to fight bacterial infections. *Biol. Targets Ther.* **2022**, *16*, 173–186. [[CrossRef](#)]
49. García-Anaya, M.C.; Sepúlveda, D.R.; Rios-Velasco, C.; Zamudio-Flores, P.B.; Sáenz-Mendoza, A.I.; Acosta-Muñoz, C.H. The role of food compounds and emerging technologies on phage stability. *Innov. Food Sci. Emerg. Technol.* **2020**, *64*, 102436. [[CrossRef](#)]
50. Jończyk-Matysiak, E.; Łodej, N.; Kula, D.; Owczarek, B.; Orwat, F.; Międzybrodzki, R.; Neuberg, J.; Bagińska, N.; Weber-Dąbrowska, B.; Górski, A. Factors determining phage stability/activity: Challenges in practical phage application. *Expert Rev. Anti-Infect. Ther.* **2019**, *17*, 583–606. [[CrossRef](#)]
51. Rode, T.M.; Axelsson, L.; Granum, P.E.; Heir, E.; Holck, A.; L'Abée-Lund, T.M. High stability of Stx2 phage in food and under food-processing conditions. *Appl. Environ. Microbiol.* **2011**, *77*, 5336–5341. [[CrossRef](#)]
52. Souza, V.G.L.; Rodrigues, C.; Valente, S.; Pimenta, C.; Pires, J.R.A.; Alves, M.M.; Santos, C.F.; Coelho, I.M.; Fernando, A.L. Eco-friendly ZnO/Chitosan bionanocomposites films for packaging of fresh poultry meat. *Coatings* **2020**, *10*, 110. [[CrossRef](#)]
53. Fox, P.; Uniacke-Lowe, T.; McSweeney, P.; O'Mahony, J.; Fox, P.; Uniacke-Lowe, T.; McSweeney, P.; O'Mahony, J. Physical properties of milk. In *Dairy Chemistry and Biochemistry*; Springer: Berlin/Heidelberg, Germany, 2015; pp. 321–343.
54. Kropinski, A.M. Practical advice on the one-step growth curve. *Bacteriophages Methods Protoc.* **2018**, *3*, 41–47.
55. Laanto, E.; Bamford, J.K.; Laakso, J.; Sundberg, L.-R. Phage-driven loss of virulence in a fish pathogenic bacterium. *PLoS ONE* **2012**, *7*, e53157. [[CrossRef](#)] [[PubMed](#)]
56. Egidio, J.E.; Costa, A.R.; Aparicio-Maldonado, C.; Haas, P.-J.; Brouns, S.J. Mechanisms and clinical importance of bacteriophage resistance. *FEMS Microbiol. Rev.* **2022**, *46*, fuab048. [[CrossRef](#)] [[PubMed](#)]
57. Yuan, Y.; Wang, L.; Li, X.; Tan, D.; Cong, C.; Xu, Y. Efficacy of a phage cocktail in controlling phage resistance development in multidrug resistant *Acinetobacter baumannii*. *Virus Res.* **2019**, *272*, 197734. [[CrossRef](#)]
58. Li, N.; Zeng, Y.; Wang, M.; Bao, R.; Chen, Y.; Li, X.; Pan, J.; Zhu, T.; Hu, B.; Tan, D. Characterization of phage resistance and their impacts on bacterial fitness in *Pseudomonas aeruginosa*. *Microbiol. Spectr.* **2022**, *10*, e02072-22. [[CrossRef](#)] [[PubMed](#)]
59. Shen, K.; Shu, M.; Zhong, C.; Zhao, Y.; Bao, S.; Pan, H.; Wang, S.; Wu, G. Characterization of a broad-spectrum endolysin rLysJNwz and its utility against *Salmonella* in foods. *Appl. Microbiol. Biotechnol.* **2023**, *107*, 3229–3241. [[CrossRef](#)] [[PubMed](#)]
60. Jiang, Y.; Xu, D.; Wang, L.; Qu, M.; Li, F.; Tan, Z.; Yao, L. Characterization of a broad-spectrum endolysin LysSP1 encoded by a *Salmonella* bacteriophage. *Appl. Microbiol. Biotechnol.* **2021**, *105*, 5461–5470. [[CrossRef](#)] [[PubMed](#)]
61. Liu, B.; Guo, Q.; Li, Z.; Guo, X.; Liu, X. Bacteriophage endolysin: A powerful weapon to control bacterial biofilms. *Protein J.* **2023**, *42*, 463–476. [[CrossRef](#)]
62. Gill, J.; Sabour, P.; Leslie, K.; Griffiths, M. Bovine whey proteins inhibit the interaction of *Staphylococcus aureus* and bacteriophage K. *J. Appl. Microbiol.* **2006**, *101*, 377–386. [[CrossRef](#)]

Disclaimer/Publisher's Note: The statements, opinions and data contained in all publications are solely those of the individual author(s) and contributor(s) and not of MDPI and/or the editor(s). MDPI and/or the editor(s) disclaim responsibility for any injury to people or property resulting from any ideas, methods, instructions or products referred to in the content.